phase; the entire specimen lights up when making a dark-field image in a superstructure spot. As a result the 400 spot (*i.e.* the $110_{f.c.c.}$ spot) is not reinforced by diffraction from a matrix, as opposed to what is almost inevitably the case in Al_5Ti_3.

The model also explains, of course, why dark-field images in the diffraction contrast mode, made in incommensurate reflections, reveal the islands as bright patches.

The size of these islands is to a large extent independent of the annealing temperature but decreases with increasing deviations from the stoichiometric composition.

A similar phenomenon was observed by some of the present authors (Den Broeder *et al.*, 1981) in Cr-Al alloys at compositions between 26 and 33 at.% Al. Here a phase called X with composition close to Cr_5Al_3 was observed which, in spite of very long annealing times, remained in an embryonic size range of 3-5 nm; the influence of composition on island size was less pronounced here.

The model also explains why even in nominally stoichiometric Al_5Ti_3 some $TiAl_2$ precipitates are still found. The stoichiometric compound only exists in small islands, the rest of the specimen contains Al_2Ti and $TiAl$; the first one contains an excess of Al whereas the second contains an excess of Ti.

When irradiating a sample containing Al_5Ti_3 islands as well as Al_2Ti precipitates in a matrix of AlTi it is found that Al_5Ti_3 is preferentially disordered. The superstructure reflections due to Al_5Ti_3 disappear rapidly whereas the diffraction spots due to the Al_2Ti and AlTi remain (Fig. 3d). These observations suggest that Al_5Ti_3 is a less stable structure than Al_2Ti and AlTi.

9. Conclusions

In the present paper we have tried to explain the incommensurability in the electron diffraction patterns by assuming a core region with structure A surrounded by a thin boundary region having a structure B. If this boundary area becomes very narrow (in terms of the unit cell which is here $1\cdot1 \times 1\cdot1$ nm) it is difficult to define the structure B and it becomes equally justified to describe the island as consisting completely of structure A but containing a single antiphase boundary close to the border. The schematic representation of Fig. 10 can be readily interpreted in this way. The diffraction effects associated with a single APB in a small crystal as well as those associated with a set of small islands all containing APB's of the same type have been extensively analyzed in a recent paper by Van Dyck *et al.* (1984).

In the particular model considered here the approach used in the present paper and that used by Van Dyck *et al.* (1984) lead to consistent results.

References

DEN BROEDER, F. J. A., VAN TENDELOO, G., AMELINCKX, S., HORNSTRA, J., DE RIDDER, R., VAN LANDUYT, J. & VAN DAAL, H. J. (1981). *Phys. Status Solidi A*, **67**, 233-248.

FUJIWARA, K. (1957). *J. Phys. Soc. Jpn*, **12**, 7-13.

LOISEAU, A. & LASALMONIE, A. (1983). *Acta Cryst* B**39**, 580-587.

LOVEY, F. C., VAN TENDELOO, G., VAN LANDUYT, J., CHANDRASEKARAN, M. & AMELINCKX, S. (1984). *Acta Metall.* **32**, 879-886.

MIIDA, R., HASHIMOTO, S. & WATANABE, D. (1982). *Jpn. J. Appl. Phys.* **21**, L59-L61.

VAN DYCK, D. (1980). *J. Microsc.* **119**, 141-152.

VAN DYCK, D., VAN TENDELOO, G. & AMELINCKX, S. (1984). *Ultramicroscopy*, **15**, 357-370.

VAN TENDELOO, G. & AMELINCKX, S. (1978). *Phys. Status Solidi A*, **47**, 555-564.

The Solution of Unknown Crystal Structures from X-ray Powder Diffraction Data. Technique and an Example, ZrNaH(PO4)2

BY PHIL RUDOLF AND ABRAHAM CLEARFIELD*

Chemistry Department, Texas A&M University, College Station, Texas 77843, USA

Abstract

An integrated system whereby the structure of an unknown polycrystalline compound can be solved from X-ray powder data, collected on a powder diffractometer, is described. The method developed falls into three main sections: accurate data collection and analysis of the pattern to give unit-cell parameters and space group; structure analysis, *via* Patterson/direct methods and Fourier/difference Fourier techniques using integrated intensities of unam-

* To whom correspondence should be addressed.

biguously indexed peaks in the pattern; and lastly a complete Rietveld refinement analysis of the entire powder profile. The method is illustrated by the solution of the crystal structure of $ZrNaH(PO_4)_2$. This compound is monoclinic with Rietveld-refined cell parameters of $a = 8 \cdot 8666$ (3), $b = 5 \cdot 3583$ (2), $c = 16 \cdot 1284$ (5) Å, $\beta = 115 \cdot 96$ (8)°; space group $P2/c$ and $Z = 4$. The Na^+ ions are in twofold special positions halfway between the α-zirconium phosphate layers. One of them is six coordinate with Na–O bond distances of $2 \cdot 29$ (9) to $2 \cdot 49$ (6) Å. The other Na^+ ion is eight coordinate with Na–O interatomic distances of $2 \cdot 63$ (7) to $2 \cdot 99$ (7) Å. The Zr–O and P–O bond distances and angles were found to be quite regular. Final agreement factors were $R_{wp} = 0 \cdot 164$, $R_F = 0 \cdot 044$ and $R_I = 0 \cdot 07$.

Introduction

Powder methods of recording X-ray diffraction patterns were developed shortly after the discovery of diffraction by crystals (Friedrich, 1913; Keene, 1913). Because of the limited amount of data available by this method and the difficulty in obtaining accurate intensities, powder data have largely been used for many purposes other than structure solutions. However, there exists a large body of crystalline materials for which single crystals are not available. Therefore it would be highly desirable if routine methods of structure solution and refinement were available using powder data.

There are many difficulties inherent in achieving this goal. Foremost among them is the ability to obtain sufficient high quality, unambiguously identified and accurately determined peak intensities. In this regard neutron data present less of a problem as the neutron peaks conform to a Gaussian shape. The advent of the Rietveld full profile refinement method (Rietveld, 1967, 1969) for neutron data has proved to be quite effective in obtaining well refined structures (Cheetham & Taylor, 1977). The weakness of the method lies in the necessity of having a relatively good starting model for the refinement.

During the past decade great progress has been made in recognizing and overcoming some of the problems that have plagued the acquisition of accurate X-ray intensities from powder data (for example: Block & Hubbard, 1980; Hubbard, Barrett, Predecki & Leyden, 1983). Furthermore, several versions of an X-ray Rietveld program are now available (Baerlocher, 1982; Wiles & Young, 1981). Recently Swedish workers (Berg & Werner, 1977) showed that the Rietveld technique could be combined with standard Patterson and Fourier techniques for the solution of completely unknown structures. Powder data were obtained with a Guinier–Hägg focusing camera with strictly monochromatic Cu $K\alpha_1$ radiation. Peak positions and integrated intensities were obtained by use

of an automated microdensitometer (Johansson, Palm & Werner, 1980). Several additional structures have been solved by this technique (Werner, 1980). However, it seemed to us that a system was needed where data could be obtained with an automated diffractometer and structures solved in semi-routine fashion. Techniques already in use include Mortier's Fourier method (Mortier & Costenoble, 1973; Pearce, Mortier, Uytterhoeven & Lunsford, 1981) and the Rietveld method (Young, 1980). The disadvantage of these methods is the necessity of having a good starting model.

In cases where the structure is unknown several methods leading to structure solutions have been employed. These include refinement based on model building (Baerlocher, 1983); structural isomorphs (for example: Thomas, 1980); isostructural compounds (Casado, Mendiola & Rasines, 1982) or new structures (for example: Smith, Maskasky & Spaulding, 1982; Nolang & Tergenius, 1980; Rossell, 1980). None of these procedures is of general applicability.

In this paper we describe a method whereby an unknown structure may be determined from X-ray diffractometer data from first principles. We have been successful in obtaining structural information in 70% of the powders examined. The power and scope of the method are yet to be fully explored as only low-symmetry examples have as yet been examined (for example: Rudolf, 1983; Clearfield, McCusker & Rudolf, 1984).

Experimental

Data collection

X-ray powder intensity data are collected on a computer-controlled vertical-reflection-mode powder diffractometer (Seifert-Scintag, PADII). The diffractometer is controlled by a microcomputer with floppy disks for temporary data storage. Samples are irradiated by means of a standard-focus Cu-target X-ray tube (Seifert, 2000 W). All diffractometer spectra are taken with Ni-filtered Cu $K\alpha$ radiation ($\lambda = 1 \cdot 54184$ Å) using a scintillation detector (Mortier, 1980). The intensity data are stored on a disk prior to transferring to larger computers for data reduction and analysis.

Internal calibration is effected with NBS standard silicon powder reference material No. 640 ($a = 5 \cdot 43088$ Å). Diffractometer data are normally collected between 5 and 80° 2θ to allow the same data to be used in all stages of the calculation. For the same reason the samples used usually contain ca 5–10% of Si calibrant to allow accurate cell-parameter determination. Counting times and step width vary with the sample but are usually either $0 \cdot 01°/36s$ or $0 \cdot 02°/72s$. This procedure is found to afford excellent data resolution, and excellent counting statistics. The

use of a crystal monochromator can aid in background and noise reduction though intensities are reduced correspondingly. Details of the diffractometer arrangement are given elsewhere (Mortier, 1980). Powder samples are usually loaded by a side-loading method to reduce in-plane preferred-orientation effects. In cases where calibrant lines overlap sample lines, separate data may be collected with calibrant for cell parameters and without calibrant for intensities.

Determination of the trial structure

After data collection the data are transferred to a PDP-11 series computer and the data formatted and reduced to a form compatible with the Nicolet powder package (Sparks, 1980) locally modified to run under RSX-11M. Data are checked for spikes and excessive noise, scaled, and smoothed as necessary. A comprehensive deconvolutory profile analysis is then conducted as reported by Sparks (1980). The individual peak profile at this stage is determined empirically from the pattern (Sparks, 1980). The resulting peak positions are corrected in 2θ by means of the internal calibrant and indexing is then performed by both the trial-and-error (Werner, 1964) and Ito (Visser, 1969) methods. Fig. 1 gives a flow diagram of the procedures from raw data to indexing. At this stage it should be
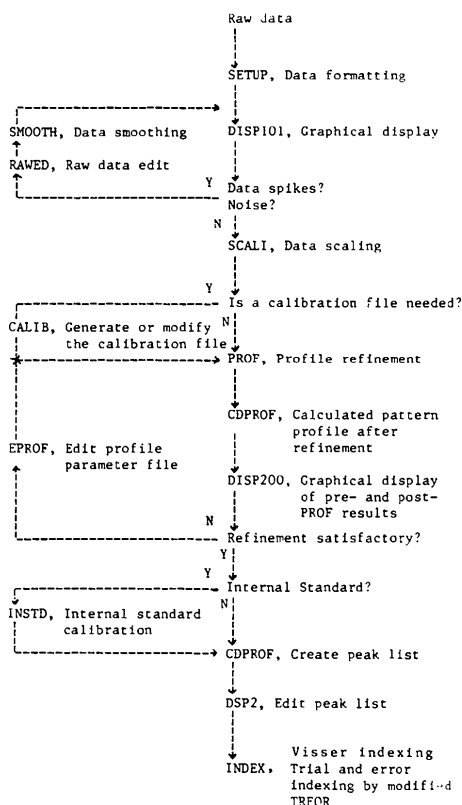

Fig. 1. Flow diagram outlining the procedure from data collection to indexing.

noted that data may need to be scaled downwards to help minimize errors occurring because of truncations in the deconvolution program PROF (Sparks, 1980). Also, careful graphical monitoring of refinement regions by visual observation on the CRT screen or hardcopy printouts helps to pinpoint extra peaks hidden in the pattern before indexing is attempted. A well refined region has an observed/calculated difference plot which is nearly flat. Unaccounted peaks are easily seen in the difference plot. After indexing, the cell volumes, crystal systems and index assignments are examined critically until reasonable values are obtained. The final assignments should show no large d_{obs}/d_{calc} discrepancy and all lines should be indexable. The cell volume should also show consistency with the formula of the compound being studied. A least-squares refinement of the unit-cell parameters is then conducted with program LSUCRE (Rudolf, 1982a) with all the resolved peak positions obtained from the deconvolution process of PROF. This refinement procedure allows poorly refined areas to be pinpointed and additional peaks included, or removed, in PROF. PROF splits the pattern into ranges and each range can hold 256 data points. Up to 15 peaks can be refined in each range. Peaks are refined on 2θ, intensity and full width at half maximum (FWHM). Each range can also have its background refined. After obtaining the most satisfactory refinement results from the full-pattern deconvolution process of PROF and the cell-parameter refinement of program LSUCRE, any peaks with ambiguous index assignments are removed and the reflection list checked for systematic absences.

Once all the unambiguous indices have been assigned, program STRUCF (Rudolf, 1982b) is run to convert the hkl and integrated I (from PROF) into a form for input to Enraf–Nonius's structure determination package, SDP (Enraf–Nonius, 1981). A flow diagram of the procedures from indexing to the SDP is given in Fig. 2.

A trial structure is now obtained by using the indexed reflection data to obtain heavy-atom positions via Patterson synthesis or MULTAN (Germain, Main & Woolfson, 1981). Normal Fourier methods are applied to locate the remaining atoms. After location of most of the atoms, a limited refinement is conducted under highly damped and constrained refinement conditions. Refinement of only a few variables at a time, consistent with the low number of data being used at this stage, is usually possible.

Final structural parameters

Upon completion of this 'Fourier refinement' both raw data and the positional parameters are transferred to a VAX 11/780 for rerefinement of the structure via the Rietveld technique. We are currently using the XRS-82 series of programs (Baerlocher, 1982) which

have been extensively modified to run under VMS. *PLOT*-10 compatible graphics have been added as has the ability to strip mathematically $K\alpha_2$ contributions and check the raw data for spikes and other errors. Atom parameters, group parameters, cell parameters, zero-point error and peak-profile parameters may all be refined with this program series.

The initial step in the use of *XRS*-82 involves formatting and stripping of $K\alpha_2$ contributions after the method of Ladell, Zagofsky & Pearlman (1975). The data are then treated to remove unwanted reflections, such as those of the calibrant. A refinement based on the full powder profile is now conducted. A flow diagram of the procedures involved is given in Fig. 3. This package has proved to be successful as refinement can be conducted on a weighted basis between the full-profile fit and known geometric constraints of the structure.

An important aspect of the Rietveld procedure is the refinement of the peak-profile parameters. In the present program eight such parameters are used, four for the lattice constants and four for the refinement of peak width and peak asymmetry as a function of 2θ. The equations for the peak refinement are as follows:

$$WD_{cor} = t \times WD_{est} + U \times 2\theta \times WD_{est} \qquad (1)$$

$$PA_{cor} = V \times PA_{est} + W \times 2\theta \times PA_{est} \qquad (2)$$

where t, U, V and W are variables and WD_{est} and PA_{est} are the estimated peak widths (FWHM) and peak asymmetries, respectively.
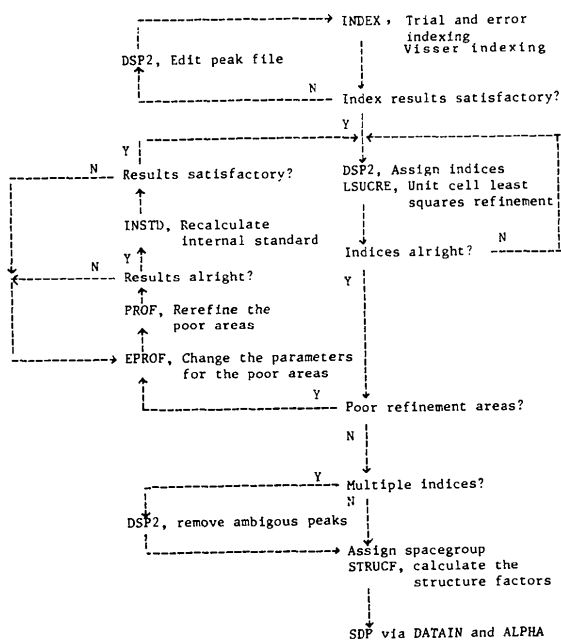
The peak-shape function used has the form (Hepp, 1981)

$$G = \left[\frac{1}{H}g_s\left(\frac{\Delta 2\theta}{H}\right)\right]\left[1 - Ag_a\left(\frac{\Delta 2\theta}{H}\right)\right] \qquad (3)$$

where H is the half width at half height and A the asymmetry parameter. The g_s and g_a are the normalized functions representing the symmetric and asymmetric parts of the peak-shape function. They are non-analytic functions for which the second derivative exists and are determined in numerical form from a single resolved peak in the experimental profile (Hepp, 1981). This procedure gives an accurate description of the actual peak shape observed as shown in Fig. 4, and eliminates the necessity of choosing an analytical function to describe the peak. The parameters H and A depend on 2θ and their dependence is determined beforehand from the observed powder pattern. In the Rietveld refinement these parameters can be adjusted according to equations (1) and (2). The adjustment of the half-width and peak-asymmetry parameters is critical in the early stages
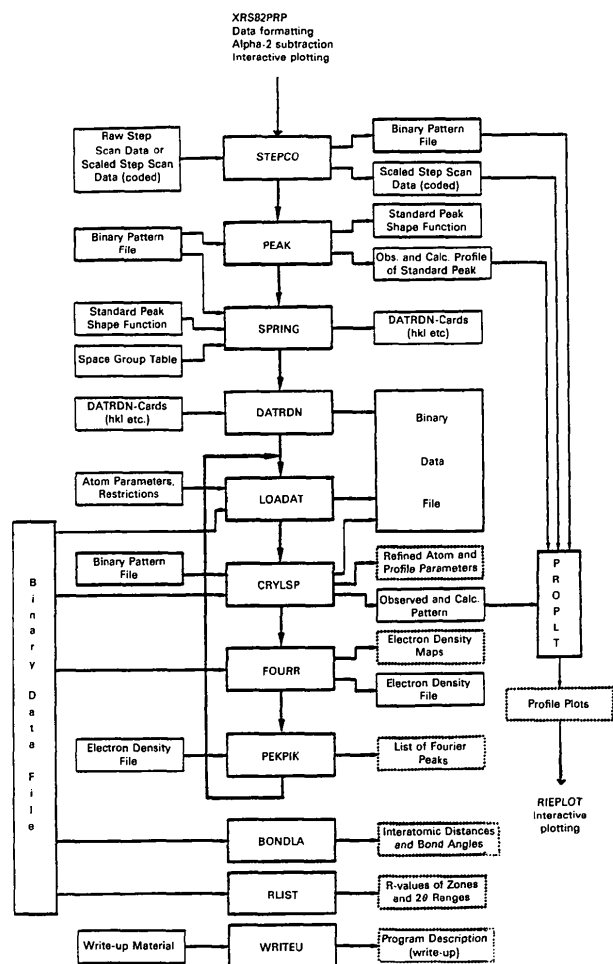

Fig. 2. Flow diagram outlining the procedure from indexing to single-crystal programs.

Fig. 3. Flow diagram for the *XRS*-82 (Rietveld) series of programs.

of refinement. Once they are correct, the structural parameter refinement converges rapidly.

In the cases studied we have found that execution time on the VAX is short (4000 data, 50 variables, 2 cycles *ca* 5 min) although each structure may require about 5000 blocks to allow for backups of previous refinement cycles. The *PLOT*-10 graphics provide for a rapid means of graphically monitoring the refinement procedure. Refinement usually converges for a set of parameters within three cycles and, if necessary, missing atoms can be found through Fourier techniques. An example of structure solution and refinement with this system is given next to illustrate the power and accuracy of the techniques outlined above.

Experimental results

Materials. α-Zirconium bis(monohydrogenorthophosphate) monohydrate, α-$Zr(HPO_4)_2.H_2O$ or α-ZrP, has layered structure as determined by a single-crystal structure solution (Troup & Clearfield, 1977). The two acidic H atoms may be ion-exchanged for Na^+ ions as previously reported (Clearfield, Duax, Medina, Smith & Thomas, 1969; Clearfield & Medina, 1970) although the partially or fully exchanged phases cannot be prepared as crystals suitable for single-crystal X-ray studies. The monosodium-exchanged form was prepared from highly crystalline microcrystalline α-ZrP and the dehydrated phase obtained by annealing at 393 K. Once the dehydrated phase, $ZrNaH(PO_4)_2$, is formed, it is stable under ambient conditions.

Data collection and structure solution. Data were collected using a side-loaded sample at the rate of 1° 2θ h^{-1} in the range 5–85°. The step width was 0·01° 2θ with a step time of 36 s.* Approximately 5% by volume NBS SRM#640 (Si powder) was added as internal calibrant. Data reduction followed by index-

---

* A listing of the collected data for each interval and a table of *d* spacings and normalized intensities for $ZrNaH(PO_4)_2$ have been deposited with the British Library Lending Division as Supplementary Publication No. SUP 42051 (18pp.). Copies may be obtained through The Executive Secretary, International Union of Crystallography, 5 Abbey Square, Chester CH1 2HU, England.
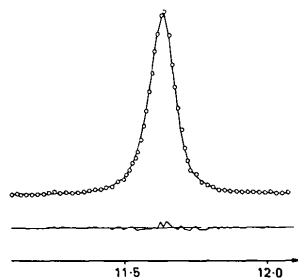

Fig. 4. Typical standard peak used as a base profile for refinement. The symbols show calculated points whilst the lower trace is the difference.

ing, as described earlier, led to 46 unambiguously indexed reflections. Unit-cell refinement using resolved peak positions and program *LSUCRE* gave the monoclinic cell parameters as *a* = 8·858 (2), *b* = 5·351 (2), *c* = 16·107 (4) Å, β = 115·93 (4)°. These dimensions are slightly smaller than the full-profile-refined data listed in Table 1 (see below). Absences of the type *h0l* with *l* = 2*n* + 1 were noted and the presence of a strong 010 peak and a possible 030 reflection showed that space groups *Pc* or *P2/c* were possible. A cell volume of *ca* 686 Å^3 gives *Z* = 4. This compares to the measured volume for $Zr(HPO_4)_2.H_2O$ of 726 Å^3 (D_{obs} = 2·72 g cm^{-3}) with *Z* = 4 (Clearfield & Smith, 1969). Solution was effected in the centrosymmetric space group.

The reflection and cell information were input into the *SDP* as a minimal data set and the resulting Patterson map yielded (from Harker sections) the position of the Zr atom. A strong vector in the Patterson map also indicated the correct position of atom P(1). The remaining atoms were found by a combination of Fourier and difference Fourier techniques. Heavily damped refinement of the structure was conducted, a few atoms at a time, to the point where R_F = 0·180 at which stage the 00*l* reflections were examined and removed from the calculations as they were seen to exhibit severe preferred-orientation effects. A factor of *ca* 2·7 existed between $F_o(00l)$ and $F_c(00l)$. Removal of these reflections together with additional refinement lowered R_F to 0·149 for 42 observations. Throughout this procedure bond lengths and angles were monitored carefully for deviation from 'acceptable' values. Although the Zr-atom parameters could be refined from the start of the procedure there were recurrent problems when trying to refine the O parameters. The refinement went well as long as not more than five variables were treated at any one time.

Full structural refinement by Rietveld technique. The structural information was now input to the *XRS*-82 series of programs. The data had the $K\alpha_2$ contribution removed and also the small regions where the Si peaks occur. Constraints were placed on the refinement in the form of known Zr–O and P–O bond distances and O–Zr–O and O–P–O bond angles. Initially the approximate atomic coordinates were refined using these constraints to obtain an idealized geometry as a starting model. As structural refinement progressed the geometric constraints were given less and less weight with respect to the X-ray data but could not be completely removed. It was also found advantageous to use only the data from 10 to 80° 2θ as the lower- and higher-angle data contained excessive noise. Both the unit-cell parameters and profile-adjusting parameters were least-squares fit to these data several times as the refinement progressed. These final cell parameters (Table 1) were slightly larger than those obtained from *LSUCRE* using the 47

Table 1. *Crystallographic data for* ZrNaH(PO₄)₂ *from Rietveld full-profile refinement*

Space group	$P2/c$, monoclinic
Z	4
a	8·8666 (3) Å
b	5·3583 (2)
c	16·1284 (5)
β	115·96 (8)°
V	688·9 Å³
D_x	2·95 g cm⁻³
No. of steps	3330
No. of reflections	366
No. of variables	46
No. of atoms	13
$R_F = \sum |F_o - F_c|/\sum F_o$	0·044 (0·043)*
$R_I = \sum |(F_o^2 - F_c^2)|/\sum F_o^2$	0·07 (0·094)
R_{wp} (profile)	0·164 (0·134)
$= \{\sum w_i[y_i(\text{obs}) - y_i(\text{calc})/c]^2/\sum w_i y_i^2(\text{obs})\}^{1/2}$	
Preferred-orientation factor	0·061
Maximum number of overlapping reflections	122
Limits of 2θ data for refinement	10°–80°

* Numbers in parentheses are statistically expected values.

Table 2. *Final positional and thermal parameters with their e.s.d.'s for* ZrNaH(PO₄)₂

The errors on all parameters have been calculated according to Scott (1983).

	x	y	z	$B(\text{Å}^2)$
Zr	0·7389 (17)	0·7665 (34)	0·9836 (7)	0·84 (27)
Na(1)	0·50	0·157 (15)	0·25	7·4 (28)
Na(2)	0·00	−0·027 (14)	0·25	
P(1)	0·162 (3)	0·725 (9)	0·117 (2)	1·0 (8)
P(2)	0·700 (3)	0·258 (9)	0·115 (2)	
O(1)	−0·012 (4)	0·724 (15)	0·045 (3)	2·5*
O(2)	0·274 (8)	0·500 (12)	0·113 (5)	
O(3)	0·256 (8)	0·956 (13)	0·104 (5)	
O(4)	0·720 (8)	0·501 (12)	0·072 (4)	
O(5)	0·492 (4)	0·784 (14)	0·923 (3)	
O(6)	0·782 (7)	0·032 (11)	0·089 (4)	
O(7)	0·178 (6)	0·727 (17)	0·217 (3)	
O(10)	0·204 (7)	0·284 (17)	0·284 (3)	

* Could not be refined.

deconvoluted reflections. Once all parameters had been refined the weighting of the constraints was released until the ratio of profile weight to geometric-constraint weight was 2·0. The last variable to refine was the preferred-orientation factor. The preferred-orientation factor used is for platy crystal forms and is calculated as $P = \exp(p \cos 2\delta)$ where p is the preferred-orientation vector and δ is the angle between the preferred-orientation vector and the scattering vector hkl. In this refinement p was 0·061. Table 1 contains a list of the final parameters and Fig. 5 is the final Rietveld difference plot.

Discussion of the results

Table 2 gives the final positional and thermal parameters and their e.s.d.'s for ZrNaH(PO₄)₂. The e.s.d.'s have been calculated as reported previously (Scott, 1983). An *ORTEP* projection (Johnson, 1965) of the structure showing two adjacent layers and the arrangement of the exchanged ions between the layers
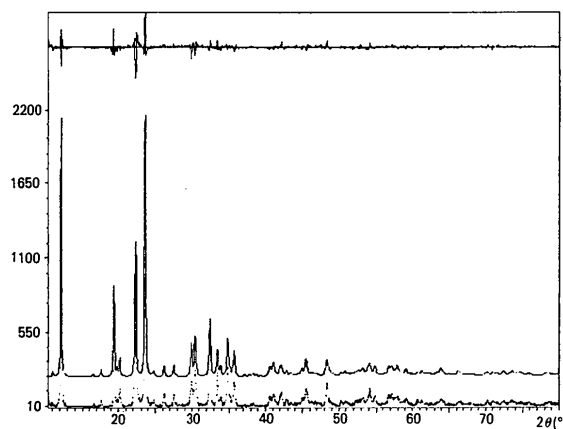
is given in Fig. 6. The structure is essentially that of the corresponding K salt reported earlier (Clearfield, McCusker & Rudolf, 1984) with the only difference being the O coordination about Na(2). Each of these Na⁺ ions has a highly distorted octahedral O coordination with bond distances of Na(2)–O(6) 2·49 (6), Na(2)–O(7) 2·29 (9) and Na(2)–O(10) 2·34 (9) Å. In the K⁺-ion structure both K⁺ ions are eight coordinate. The difference results from the fact that in the K⁺-ion structure the O atoms which were originally bonded to protons in Zr(HPO₄)₂.H₂O [O(7) and O(10)] are located at approximately $x = \frac{1}{4}$ or half way between K atoms. In the present structure they are moved towards lower x values and thus make unequal interatomic distances to the two Na⁺ ions. Na(1) which is at $x = \frac{1}{2}$ is thus surrounded by six lattice O atoms (those bonded to both Zr and P) at long distances: Na(1)–O(2) 2·90 (8), Na(1)–O(3) 2·63 (7) and Na(1)–O(5) 2·84 (8) Å. O(10) then completes the coordination at a long distance of 2·99 (7) Å.
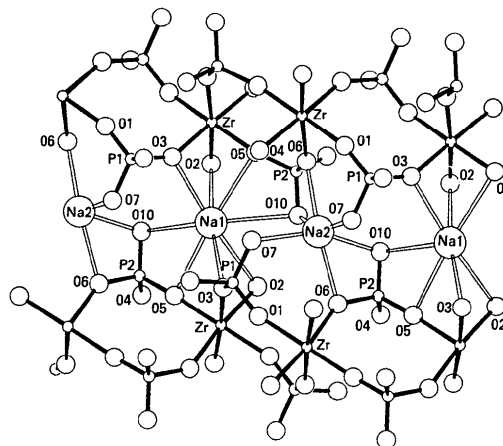

Fig. 5. Final Rietveld difference plot. Observed pattern, lower; calculated, middle; and difference, top.

Fig. 6. *ORTEP* projection of the refined structure showing the exchange-ion coordination. a is horizontal and c vertical (at 116° to a).

Table 3. *Comparison of average bond lengths (Å) and angles (°) and their e.s.d.'s*

E.s.d.'s are calculated as $[\sum (ave - obs)/N(N-1)]^{1/2}$.

	Single-crystal refined*	Rietveld refined†	Parent α-ZrP‡
Zr–O	2·199 (78)	2·049 (23)	2·065 (5)
P(1)–O	1·607 (81)	1·541 (24)	1·528 (13)
P(2)–O	1·572 (36)	1·530 (19)	1·526 (18)
O–Zr–O	89·0 (40)	90·0 (10)	90·0 (2)
O–P(1)–O	107·8 (50)	109·2 (20)	109·5 (13)
O–P(2)–O	109·0 (54)	109·5 (18)	109·2 (12)
Zr–O–P	146·4 (61)	153·0 (52)	150·8 (27)
Zr–O (range)	1·96–2·50ˆ	1·969–2·117	2·048–2·075
P–O (range)	1·42–1·81	1·470–1·562	1·510–1·564

* Based on 42 reflections.
† Final parameters from full-profile refinement.
‡ From Troup & Clearfield (1977).

Table 3 lists the average bond lengths and angles for this structure, both for the trial structure derived from the 'Fourier refinement' of 42 well resolved reflections (Rudolf, 1983) and the Rietveld-refined structure. Similar data derived from a single-crystal study of the parent α-ZrP are also presented here. Comparison of the two results shows that, within error limits, the Rietveld-refined and 42-reflection structure are the same. However, the range of bond distances obtained in the Fourier refinement is much larger and obscures the fine detail of the structure. Comparison with the values derived for α-ZrP shows the plausibility of the bond lengths, angles and e.s.d.'s for the Rietveld-refined structure.

Recent results from EXAFS studies (Alagna & Tomlinson, 1982) indicate that the Cu^{II} ion in $ZrCu(PO_4)_2$ has a tetragonally distorted octahedral $CuO_4 + 2O$ coordination. The four Cu–O distances average 1·923 (10) Å and conform roughly to square-planar geometry. These O atoms were found to arise from four different phosphate groups with the P atoms at 2·48 Å from the Cu^{2+}. It was postulated that both a sliding and 10° rotation of adjacent layers was necessary to achieve this geometry. The coordination about Na(2) in the present structure approximates this geometry. The Na^+ radius is about 0·25 Å larger than that of Cu^{2+} so the Na–O bond distances should be approximately 2·2 Å on the Alagna–Tomlinson model and the P atoms at 2·73 Å (second EXAFS shell) from the Na^+ ion. Actually this latter distance is 3·02 Å. Thus, the EXAFS results for Cu^{II} are not appreciably different from the present Na(2) ion coordination, which is achievable not by rotation of adjacent layers but principally by a shift of $\frac{1}{2}b$ in adjacent layers.

There is no clear indication where the remaining proton resides. O(7) is not bridging as in the K^+ structure and it would be tempting to place it there. However, the bridging O(10) forms one short bond to Na(2) and one long one (2·99 Å) to Na(1) while the O(1)–Na(2) bond is short. Thus, it is likely that the H^+ is statistically distributed between these two O atoms. It may now be possible to decide this question from a neutron diffraction study.

Concluding remarks

We have described a unified, convenient system for the determination of unknown crystal structures from diffractometer-based X-ray powder data. It might be argued that in the present case the structure was not totally unknown since the structure of the parent acid, $Zr(HPO_4)_2.H_2O$, was previously determined. However, the procedures were followed as though nothing was known about the structure. What is significant is that the Zr and P atoms could be identified in the Patterson map using 40–50 reflections. It will also be shown in subsequent publications that this is fairly general and that direct methods can be used as well. The main problem is that of indexing, and in the monoclinic and hexagonal systems we have been successful in three out of four attempts. Once indexing is accomplished the space group can usually be identified, though this is more problematic in high-symmetry cases. It now remains to explore the power and generality of the method. However, we have used the technique in several other ways. In our work on solid electrolytes where the basic framework structure is known, we were able to determine site occupancy of the conducting ions (Subramanian, Rudolf & Clearfield, 1985). In addition it was possible to obtain information on stoichiometry of the crystalline phases, particularly the number of ions in conduction sites, by refinement of occupancy factors. Finally, we were able to provide an excellent starting model for the refinement of neutron diffraction data for a non-stoichiometric form of NASICON with general formula $Na_{1+x+4y}Zr_{2-y}Si_xP_{3-x}O_{12}$ (Rudolf, Subramanian & Clearfield, 1985). Even this limited experience is sufficient to envision a large number of similar applications to many areas of chemistry, physics, ceramics and materials science.

References

ALAGNA, L. & TOMLINSON, A. A. G. (1982). *J. Chem. Soc. Faraday Trans.* 1, pp. 3009–3018.

BAERLOCHER, CH. (1982). *The X-ray Rietveld System*, version of September 1982. Institut für Kristallographie und Petrographie, ETH, Zürich, Switzerland.

BAERLOCHER, CH. (1983). *Proceedings of the Sixth International Conference on Zeolites.* London: B. Herworths.

BERG, J. E. & WERNER, P. E. (1977). *Z. Kristallogr.* **145**, 310-320.

BLOCK, S. & HUBBARD, C. R. (1980). Editors. *Natl Bur. Stand. (US) Spec. Publ.* 567.

CASADO, A. G., MENDIOLA, A. & RASINES, I. (1982). *Inorg. Chem.* **21**, 2902-2903.

CHEETHAM, A. K. & TAYLOR, J. C. (1977). *J. Solid State Chem.* **21**, 253-257.

CLEARFIELD, A., DUAX, W. L., MEDINA, A. S., SMITH, G. D. & THOMAS, J. R. (1969). *J. Phys. Chem.* **73**, 3424-3430.

CLEARFIELD, A., MCCUSKER, L. B. & RUDOLF, P. (1984). *Inorg. Chem.* **23**, 4679-4682.

CLEARFIELD, A. & MEDINA, A. S. (1970). *J. Inorg. Nucl. Chem.* **32**, 2775-2780.

CLEARFIELD, A. & SMITH, G. D. (1969). *Inorg. Chem.* **8**, 431-436.

Enraf-Nonius (1981). *Structure Determination Package (SDP),* Delft, Holland.

FRIEDRICH, W. (1913). *Phys. Z.* **14**, 317-319.

GERMAIN, G., MAIN, P. & WOOLFSON, M. M. (1971). *Acta Cryst.* **A27**, 368-376.

HEPP, A. (1981). PhD Thesis, Univ. of Zürich.

HUBBARD, C. R., BARRETT, C. S., PREDECKI, P. K. & LEYDEN, D. E. (1983). Editors. *Advances in X-ray Analysis,* Vol. 26. New York: Plenum.

KEENE, H. B. (1913). *Nature (London),* **91**, 607.

JOHANSSON, K. E., PALM, T. & WERNER, P. E. (1980). *J. Phys. E,* **13**, 1289-1291.

JOHNSON, C. K. (1965). *ORTEP.* Report ORNL-3794. Oak Ridge National Laboratory, Tennessee.

LADELL, J., ZAGOFSKY, A. & PEARLMAN, S. (1975). *J. Appl. Cryst.* **8**, 499-506.

MORTIER, W. J. (1980). *Natl Bur. Stand. (US) Spec. Publ.* 567, pp. 315-323.

MORTIER, W. J. & COSTENOBLE, M. L. (1973). *J. Appl. Cryst.* **6**, 488-490.

NOLANG, B. I. & TERGENIUS, L.-E. (1980). *Acta Chem. Scand. Ser. A,* **34**, 311-312.

PEARCE, J. R., MORTIER, W. J., UYTTERHOEVEN, J. B. & LUNSFORD, J. H. (1981). *J. Chem. Soc., Faraday Trans.* 1, pp. 937-946.

RIETVELD, H. M. (1967). *Acta Cryst.* **22**, 151-152.

RIETVELD, H. M. (1969). *J. Appl. Cryst.* **2**, 65-71.

ROSSELL, H. J. (1980). *Nature (London),* **283**, 282-283.

RUDOLF, P. R. (1982a). *LSUCRE.* Program for least-squares unit-cell refinement. Univ. Frieberg, 1972. Modified Texas A&M, 1982.

RUDOLF, P. R. (1982b). *STRUCF.* Program for structure factor calculation. Texas A&M Univ., 1982.

RUDOLF, P. R. (1983). PhD dissertation, Texas A&M Univ.

RUDOLF, P. R., SUBRAMANIAN, M. A. & CLEARFIELD, A. (1985). *Mater. Res. Bull.* In the press.

SCOTT, H. G. (1983). *J. Appl. Cryst.* **16**, 159-163.

SMITH, D. E., MASKASKY, J. E. & SPAULDING, L. R. (1982). *J. Appl. Cryst.* **15**, 488-492.

SPARKS, R. A. (1980). Presented at the 29th Annual Conference on Applications of X-ray Analysis, Denver, CO, August 1980.

SUBRAMANIAN, M. A., RUDOLF, P. R. & CLEARFIELD, A. (1985). *J. Solid State Chem.* Submitted.

THOMAS, J. O. (1980). *J. Appl. Cryst.* **13**, 605-607.

TROUP, J. M. & CLEARFIELD, A. (1977). *Inorg. Chem.* **16**, 3311-3314.

VISSER, J. W. (1969). *J. Appl. Cryst.* **2**, 89-95.

WERNER, P. E. (1964). *Z. Kristallogr.* **120**, 375-387.

WERNER, P. E. (1980). *Natl Bur. Stand. (US) Spec. Publ.* 567, pp. 503-509.

WILES, D. B. & YOUNG, R. A. (1981). *J. Appl. Cryst.* **14**, 149-151.

YOUNG, R. A. (1980). *Natl Bur. Stand. (US) Spec. Publ.* 567, pp. 143-163.

The Effects of Extinction on the Refined Structural Parameters of Crystalline BeO: a Neutron and γ-Ray Diffraction Study

BY J. W. DOWNS

Department of Geology and Mineralogy, The Ohio State University, Columbus, Ohio 43210, USA

F. K. ROSS

University of Missouri, Research Reactor, Columbia, Missouri 65211, USA

AND G. V. GIBBS

Department of Geological Sciences, Virginia Polytechnic Institute and State University, Blacksburg, Virginia 24061, USA

Abstract

Neutron and γ-ray diffraction data collected from the same single crystal of BeO were used in conventional crystal structure refinements. The very severely extinguished neutron data are adequately modeled with the Becker–Coppens anisotropic-extinction formalism. Although the thermal parameters are unreliable, the positional parameter is close to the best estimate obtained from the γ-ray results. The γ-ray (103 keV) data are much less extinguished than the neutron data. Refinements utilizing high-order γ-ray data with neutral-atom and spherical generalized scattering factors are virtually identical.